Hyperbranched polyphthalocyanine micelles with dual PTT/PDT functions for bacteria eradication under NIR window

Ying Du [a], Guangyu Chu [b], Rui Yu [c], Rui Cui [a], Yuling Wang [a], Yiyong Mai [a], Ming Guan [b,*], Fugui Xu [a,*], Yongfeng Zhou [a,*]

[a] School of Chemistry and Chemical Engineering, Frontiers Science Center for Transformative Molecules, Shanghai Jiao Tong University, 800 Dongchuan Road, Shanghai 200240, China
[b] Department of Orthopedic Surgery, The First Affiliated Hospital, Zhejiang University School of Medicine, Hangzhou 310003, China
[c] Department of Human Biology, University of Toronto Scarborough campus Toronto, Ontario, Canada

1. Experimental section

1.1 Materials

4-Nitrophthalonitrile were purchased from Adamas; Triethylene glycol were purchased from Macklin; potassium carbonate was purchased from Sinopharm Chemical Reagent. Dimethylformamide (DMF), dichloromethane (DCM), acetone, petroleum ether, methyl alcohol, tetrahydrofuran was purchased from Greagent; dimethyl sulfoxide (DMSO) was purchased from Adamas. 1,8-Diazabicyclo [5.4.0]-7-Undecene (DBU) were purchased from Adamas. 1,3-diphenylisobenzofuran (DPBF) was purchased from bidepharm; 4-dimethylaminopyridine (DMAP) was purchased from TCI; 1-(3-Dimethylaminopropyl)-3-ethylcarbodiimide hydrochloride (EDCI) was purchased from Aladdin; Vitamin c (Vc) was purchased from Aladdin Reagent Co., Ltd (Shanghai, China); the dialysis tube was made of regenerated cellulose membrane (MWCO = 3500 Da) from Greenbird (Shanghai); Methicillin-resistant Staphylococcus aureus (MRSA, ATCC43300) were courtesy of the Lab of Microbiology at the author's institute. 2',7'-dichlorofluorescein diacetate (DCFH-DA) dye and CCK-8 kit were purchased from Sigma-Aldrich (St. Louis., MO, USA). LIVE/DEAD BacLight Bacterial Viability kit was purchased from Thermo Fisher Scientific (Waltham, MA, USA). The cellular morphology was visualized using a confocal laser scanning microscope (CLSM, Olympus FV3000, Japan). The laser source (FC-808-1500-MM 201026-R441339) was purchased from SFOLT (Shanghai).

1.2 The synthesis of CNPTEG
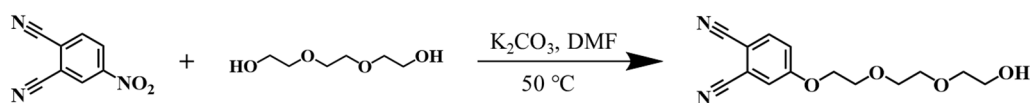
Scheme S1. The synthesis route toward CNPTEG.

The CNPTEG was synthesized according to previous report (Scheme 1).[1] Typically, 4-nitrophthalonitrile (10.0 g, 57.8 mmol), triethylene glycol (31.8 mL, 238.0 mmol) and potassium carbonate (16.0 g, 115.8 mmol) was dissolved in 115 mL DMF. The mixture was stirred at 50 °C. The reaction was monitored by thin-layer chromatography and stopped when the reactant of 4-nitrophthalonitre disappeared. After the reaction finished, 200 mL DCM was added to the mixture solution. The resultant mixture solution was washed with saturated NaCl solution (100 mL) for three times. Then, the organic phase was collected and concentrated. The crude product was purified *via* the column chromatography using acetone/petroleum ether (1:2, v/v) as eluent. After collecting and concentrated, the desired product was obtained (9.6 g, 60.0 %).

1.3 The synthesis of ZnPc-TEG
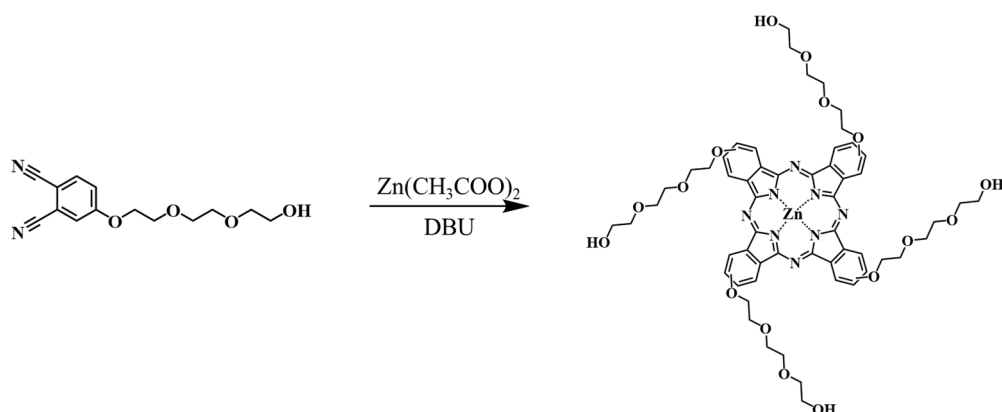
Scheme S2. The synthesis route toward ZnPc-TEG.

The ZnPc-TEG was prepared according to previous report.[1] The synthesis route toward ZnPc-TEG is shown in Scheme S2. Typically, CNPTEG (2.8 g, 10.1 mmol) was

dissolved in 100 mL n-pentanol. The mixture was stirred at 90 °C under N_2 atmosphere for 30 minutes. Then $Zn(CH_3COO)_2$ (2.2 g, 10.0 mmol), a drop of DBU was added into the mixed solution. The final mixture was stirred at 140 °C for 16 h. After the reduced pressure distillation, the crude green product was obtained. The mixture was then purified by silica gel column chromatography using THF/MeOH (10:1, v/v) as eluent. The desired product was obtained (0.4 g, 13.5%).

1.4 The synthesis of ZnPc-PA
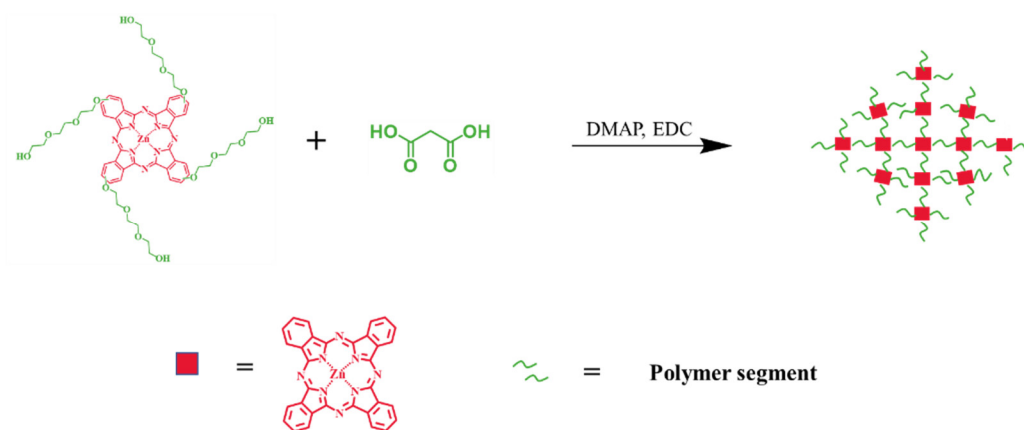
Scheme S3. The synthesis route toward ZnPc-PA.

ZnPc-PA was synthesized by "A_2+B_4" polymerization using ZnPc-TEG as B_4 monomer and propane diacid (PA) as A_2 monomer. ZnPc-TEG (584.0 mg, 499.8 mmol), propane diacid (104.0 mg, 999.7 mmol), DMAP (12.2 mg, 99.9 mmol), EDCI (1.0 g, 5.2 mmol) was dissolved in 15 mL DMF at 0 °C for 2 h and then stirred for 48 h. The mixture was purified by dialysis against DMF for three days.

1.5 Preparation of hyperbranched phthalocyanine polymer micelles

ZnPc-PA (10 mg) was dissolved in 5 mL DMSO. Then the solution was filtered by PTFE syringe filter (0.22 μm). The self-assembly of hyperbranched phthalocyanine polymer was induced by direct dialysis against the selective solvent (deionized water).

The assemblies were further dialyzed against deionized water for three days to remove DMSO.

1.6 Molecular Dynamics Simulation

The GAFF force field[2] was generated by Sobtop (http://sobereva.com/soft/Sobtop) for ZnPc-PA. And Tip3p model was used for water. The system containing 9 ZnPc and 10500 water molecules, was built by Packmol package[3]. All simulations were performed using GROMACS package[4] under the condition of three-dimensional periodic boundary. The Nosé−Hoover thermostat[5] and the Parrinello−Rahman barostat[6, 7] were employed to control the temperature and pressure. The time step of the simulation was 1 fs. After energy minimization by steepest descent algorithm, an equilibration NPT simulation was performed for 100 ns at 300 K and 1 bar.

1.7 Photothermal performance of ZnPc-PA micelles

Typically, 0.2 mL ZnPc-PA micelle solution at different concentrations (3 μM, 5 μM, 10 μM, and 20 μM) were placed in 1 mL transparent plastic centrifugal tubes. These samples were then irradiated using an 808 nm laser with an intensity of 1200 mW/cm^2. Additionally, ZnPc-PA micelles with a concentration of 20 μM was tested under various laser intensities, including 600 mW/cm^2, 900 mW/cm^2, 1200 mW/cm^2 and 1500 mW/cm^2. To measure the temperature rise during laser irradiation, a thermal imaging camera was employed. The camera recorded the thermal changes in the samples as they were exposed to the laser.

Furthermore, to assess the photothermal stability of ZnPc-PA, the samples with a concentration of 20 μM were subjected to laser irradiation at 1200 mW/cm^2, and the

heating and subsequent cooling processes were repeated three times. The photothermal

conversion efficiency (η) was calculated according to the literature.[8, 9]

The detailed calculation process was listed as follow:

$$\eta = \frac{hA(T_{max}-T_{sur})-Q_{in}}{I(1-10^{-A_{808}})} \tag{1}$$

$$hA = \frac{m_D c_D}{\tau_s} \tag{2}$$

$$t = -\tau_s \ln(\theta) \tag{3}$$

$$\theta = \frac{T-T_{sur}}{T_{max}-T_{sur}} \tag{4}$$

$$Q_{in} = hA(T_{max,H2O} - T_{sur}) \tag{5}$$

In these equations, m_D represents the weight of the sample. c_D is specific heat

capacity of water (4.2 J g^{-1} °C^{-1}). T_{max} represents the maximum temperature of sample

(56.1 °C). T_{sur} is the surrounding temperature (25.0 °C). $T_{max,H2O}$ denotes the

maximum temperature of water (26.1 °C). τ_s is the thermal equilibration time constant

that can be calculated by linear fitting. h represents the heat transfer coefficient. A

represents the surface area of the container. hA can be calculated by (2). I denotes the

laser intensity. A_{808} is the absorption intensity of ZnPc-PA micelle solution at 808 nm

(0.30).

1.8 Photodynamic measurement of the ZnPc-PA micelles and micellar-free ZnPc-PA solution

To verify the photodynamic effect of ZnPc-PA micelles, reactive oxygen species

were detected under 808 nm irradiation. The DPBF was used as a $^1O_2$ probe to identify

the kind of ROS. Typically, the absorptions of the DPBF in ZnPc-PA micelle solution

were record by UV-vis spectra with or without the 808 nm laser irradiation at different

time (0, 3, 6, 9, 12, 15 min). To identify the ability of both free ZnPc-PA and ZnPc-PA

micelles to generate specific ROS, the singlet oxygen generation quantum efficiencies

(Φ_Δ) were measured by using different references in organic and aqueous phases

respectively. 1,3-Diphenylisobenzofuran (DPBF) was used as the $^1O_2$ scavenger. The excitation wavelength of the samples was set at 808 nm.[10, 11]

In this case, the $^1O_2$ generation of ZnPc-PA micelle solution upon 808 nm irradiation was measured by using Rose Bengal (RB, $\Phi_\Delta(H_2O) = 0.75$) as a reference. And the $^1O_2$ generation of ZnPc-PA in DMF upon 808 nm irradiation was measured by using ZnPc ($\Phi_\Delta(DMF) = 0.56$) as a reference. The calculation process was listed as follows:

The calculation process was listed as follow:

$$\Phi_\Delta = \Phi_{\Delta ref} \times \frac{m}{m_{ref}} \times \frac{F_{ref}}{F} \tag{1}$$

$$F = 1 - 10^{-A} \tag{2}$$

In the equations, $\Phi_{\Delta ref}$ represents singlet oxygen generation quantum efficiency of the reference sample. F represents the absorption correction factor. m represents the slope that is calculated by the curve of DPBF absorbance versus irradiation time. A is absorbance at the irradiation wavelength (ZnPc: $A_{808} = 0.021$; Rose Bengal: $A_{808} = 0.020$; free ZnPc-PA in DMF: $A_{808} = 0.019$; ZnPc-PA micelle solution: $A_{808} = 0.21$).[12]

1.9 Cytotoxic evaluation

Cytotoxic evaluation was performed using the human endothelial cell line ECV304 cells to assess the impact of ZnPc-PA micelles. The cytotoxicity was determined using CCK-8 (Cell Counting Kit-8) assays. In brief, ECV304 cells were seeded at a concentration of 1×10^4 cells/well in a 96-well plate. The cells were then treated with various concentrations of ZnPc-PA micelles (3 μM, 5 μM, 10 μM, 20 μM) for 24 hours. A control group treated with PBS was also included. After two washes with fresh PBS, the cells were stained with a 10% CCK-8 solution for 4 hours. The relative cell density was measured using a microplate reader at a wavelength of 450 nm.

To evaluate the morphological changes of ECV304 cells following co-cultivation with PBS and ZnPc-PA micelles, cytoskeleton staining was performed. ECV304 cells were seeded at a concentration of 1×10^5 cells/well in a 24-well plate and cultured with

PBS (as the control) and ZnPc-PA micelles (at a concentration of 20 μM) for 24 hours. After being washed three times with PBS, the cells were fixed in 4% paraformaldehyde. Then, they were permeabilized using 0.1% Triton X-100 for 10 minutes. Subsequently, the cells were stained with F-actin solution (at a concentration of 30 μL mL^{-1}) to label the actin cytoskeleton for 30 minutes. The nucleus was stained with DAPI (1:1000 v/v) for 10 minutes. Finally, the cellular morphology was visualized using a confocal laser scanning microscope.

1.10 Analyzing Multidrug-resistance Bacterial Treatment Activity

Methicillin-resistant Staphylococcus aureus (MRSA) was selected as model bacterium. As note, single colony was transplanted into tryptic soy broth (TSB) and grown overnight at 37 °C. The cultures were then harvested, centrifuged, and adjusted to a 0.5 McFarland standard, corresponding to approximately $\times 10^8$ CFU/mL, using fresh TSB.

The antimicrobial efficacy *in vitro* of ZnPc-PA micelles against MRSA was evaluated using the spread plate method. Initially, 10 μL of the prepared MRSA suspension was mixed with 1 mL PBS (as control), ZnPc-PA micelles (20 μM) in 1.5 mL centrifuge tubes with or without 808 nm NIR laser (1200 mW/cm^2) for 10 min. Subsequently, 10 μL of the serially diluted bacterial solution was spread onto sheep blood agar (SBA) plates and incubated overnight at 37 °C. The bacterial colonies were then counted, and bacterial viability was calculated using the following equation:

$$\text{Bacterial Viability (\%)} = \text{E/C} \times 100\%$$

where C represents the *colony forming units* (CFUs) in the control group, and E represents the CFUs in the experimental groups. All experiments were repeated 5 times.

To visualize the morphology changes of bacteria after the aforementioned treatments, the treated bacteria were fixed with a 2.5% glutaraldehyde solution at 4 °C overnight. The fixed bacteria were then dehydrated using a series of ethanol dilutions (30, 50, 70, 85, 90, 95 and 100%, v/v) for 10 min each, following standard procedures. Subsequently, 5 μL of the suspension was transferred onto a silicon slice and freeze-dried for 24 hours. Finally, scanning electron microscope (SEM) observation was performed using a ZEISS Gemini SEM 300 microscope.

1.11 Assessing anti-biofilm Efficiency *in vitro*

A sterile pure titanium disk (Φ10 mm) was immersed in 2 mL of fresh TSB medium containing 10 μL of the prepared MRSA culture and co-incubated for 48 hours at 37 °C to allow biofilm formation on the surface of the disk. Then, the titanium disk was gently rinsed twice with aseptic PBS. Subsequently, the disk was immersed in 1 mL of PBS (control) or ZnPc-PA (at a concentration of 20 μM) under NIR laser irradiation (1200 mW/cm^2) for 5 minutes. After treatment, the titanium disk was rinsed twice with PBS to remove non-adherent bacteria and debris.

To quantitatively analyze the anti-biofilm rate, the bacteria on the surface of the titanium disk were unloaded by subjecting the disk to ultrasonic vibration for 5 minutes. The spread plate method, as described earlier, was then performed to count the colony-forming units (CFUs) in each group. The anti-biofilm rate was calculated using the following equation:

$$\text{Anti-biofilm rate (\%)} = (C-E)/C \times 100\%$$

where C and E represent the CFUs in the control group and experimental groups, respectively. All experiments were repeated 5 times. 0.1% (w/v) crystal violet was used

to stain the biofilms for 2 minutes. The biofilms were then washed once with distilled water and dried at 37 °C for 15 minutes. The stained biofilms were further treated with 100 μL of 70% (v/v) ethanol to release the stain. The amount of released stain was quantified by measuring the absorbance at 590 nm using a microplate reader.

The biofilms on the titanium disks were visualized by scanning electron microscopy (SEM) after dehydration and freeze-drying, following the protocol mentioned earlier.

1.12 Subcutaneous implant-associated infection (IAI) model

All animal experimental procedures were conducted in compliance with guidelines and approved by the Ethics Committee of the First Affiliated Hospital of Zhejiang University School of Medicine (No. 20221544). Thirty male SD rats weighing approximately 250 g were used. Prior to surgery, the rats were anesthetized by intraperitoneal injection with 4% pentobarbital, and the dorsal hair was shaved. After disinfecting the exposed area, a 1 cm midline incision was made, and a subcutaneous implant consisting of a titanium disk (Φ10 mm × 0.5 mm) was placed. Each titanium disk was then incubated with 10 μL of the prepared MRSA culture at a dose of 2×10^6 CFUs mL^{-1}. The incision was sutured, and the rats were kept in a pathogen-free environment for 3 days before treatments.

The rats were randomly divided into six groups: NIR (+) groups: PBS (control) and ZnPc-PA micelles (20 μM) groups; NIR (-) groups: PBS (control) and ZnPc-PA (20 μM). A total of 50 μL of the respective samples were injected subcutaneously with or without NIR laser irradiation (1200 mW/cm^2) for 5 minutes, and the local temperature changes were recorded. On day 7 after treatments, the titanium disks were retrieved,

and the peri-implant tissues were harvested for further morphological, microbiological, and histological evaluation.

To assess the therapeutic effect of ZnPc-PA micelles for subcutaneous IAI, the general view of the dorsal skin at the implantation area was photographed before implant removal on day 7 after treatments. The presence of anti-biofilm on the implant surface was evaluated using the spread plate method and SEM after the retrieval of the implant. The biofilm on the titanium disks was fixed with 2.5% glutaraldehyde solution at 4 °C overnight, sequentially dehydrated in a series of ethanol dilutions for 10 minutes, and then freeze-dried for 24 hours before SEM observation. After capturing SEM images, the MRSA cells in the images were pseudo-colored yellow using ImageJ software for better contrast. The peri-implant tissues were harvested and divided into two pieces. One half of the sample was ground in 2 mL of PBS, and the homogenate was spread on sheep blood agar (SBA) plates after serial dilution for antibacterial evaluation. The other half was fixed in 4% formalin solution, embedded in paraffin, sectioned into slices, and stained with H&E and Giemsa staining for evaluation of inflammation and bacterial colonization.

1.13 Assessing the tissue damage of the surrounding tissues following irradiation

To investigate whether laser-activated ZnPc-PA micelle would cause damage to healthy tissues, we injected 200 μL ZnPc-PA micelle solution (20 μM) subcutaneously into rats and then treated with 808 nm laser at 1200 mW/cm^2 for 5 min. Then, the local skins were harvested on day 1, 3 and 7 after treatment and prepared for H&E staining.

1.14 Assessing the contribution of PDT/PTT to the antimicrobial activity

To investigate the photocytotoxicity of ZnPc-PA micelles on MRSA, bacteria solution (10^6 CFU/mL) were mixed with different concentrations of ZnPc-PA micelles (3, 5, 10, 20, 25 μM) in tube and irradiated with 808 nm laser at 1.2 W/cm^2 for 5 min. Only laser treatment was used as a control. Bacterial viability was quantitatively analyzed using the CFU counting method. To determine the contribution of each PDT/PTT to the antimicrobial activity, bacteria were cultured at 4 °C to minimize the PTT effects; Vc (2×10^{-3} M), a ROS scavenger, was added into the mixture to minimize the PDT effects.

2. Characterizations

¹H nuclear magnetic resonance measurements were performed on AVANCE III HD 400 (Bruker, Germany) spectrometer using deuterium dimethyl sulfoxide (DMSO-d_6) or $CDCl_3$ as solvent at 20 °C. **Matrix-assisted Laser Desorption and Ionization Time-of-flight Mass Spectrometry (MALDI-TOF MS)** was performed on an autoflex speed TOF/TOF (Bruker, Germany) using α-Cyano-4-hydroxycinnamic acid (HCCA) or trans-2-[3-(4-tert-Butylphenyl)-2-methyl-2-propenylidene] malononitrile (DCTB) as matrix. **Gel Permeation Chromatography (GPC)** was performed on was a Perkin-Elmer series 200 system equipped with a refractive index (RI) detector. DMF was used as the eluent at a flow rate of 1 mL/min at 70 °C. The reference sample was polymethyl methacrylate. **Dynamic Light Scattering (DLS)** was recorded on a Nanoparticle Size and Zeta Potential Analyzer ZS90 (Malvern Instruments Ltd, UK) with a 4.0 mW laser ($\lambda = 633$ nm). The measurements were conducted at 25 °C at a scattering angle of 90°. The CONTIN program was used for the processing of the data. **UV-Vis absorption spectra** were tested on a UV-Vis absorption spectrometer Lambda 35 (Perkin Elmer, Inc., USA). **Fluorescence Emission Spectra** were characterized on FLS1000 steady stated & time-resolved fluorescence spectrofluorometer. **Transmission Electron Microscope** was performed with a biotype transmission electron microscope Tecnai G2 (Thermofisher, USA). The sample was prepared by dropping on 200-mesh carbon-coated copper grids and then air-dried. **Powder X-ray diffraction spectrum** was measured on X-Ray Diffractometer D8 Advance (Bruker, Germany). The sample was prepared by vacuum freeze-drying. **The temperature variation** was recorded on the

thermal imaging camera (FOTRIC220s, China). The absorbance was measured by

using a microplate reader (Powerwave; BioTek Instruments, Winooski, VT, USA).

3 Characterization results
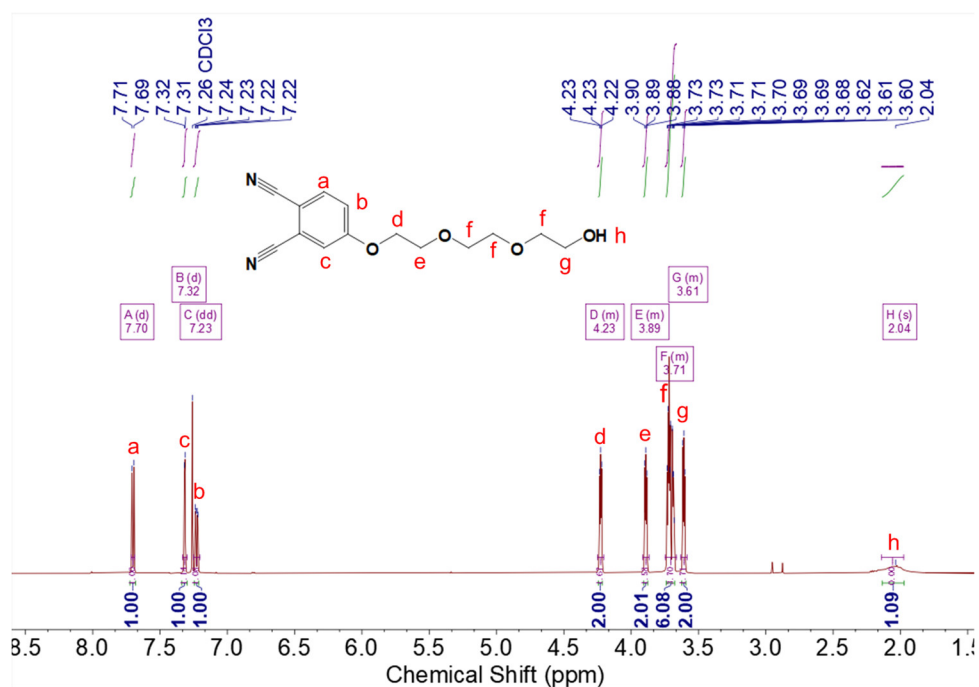
Figure S1. The ^{1}H NMR spectrum of CNPTEG (CDCl$_3$, 400 MHz).

^{1}H NMR (400 MHz, CDCl$_3$): δ 7.70 (d, J = 8.7 Hz, 1H), 7.32 (d, J = 2.6 Hz, 1H), 7.23 (dd, J = 8.8, 2.6 Hz, 1H), 4.25 – 4.20 (m, 2H), 3.91 – 3.87 (m, 2H), 3.75 – 3.66 (m, 6H), 3.63 – 3.58 (m, 2H), 2.03 (s, OH).
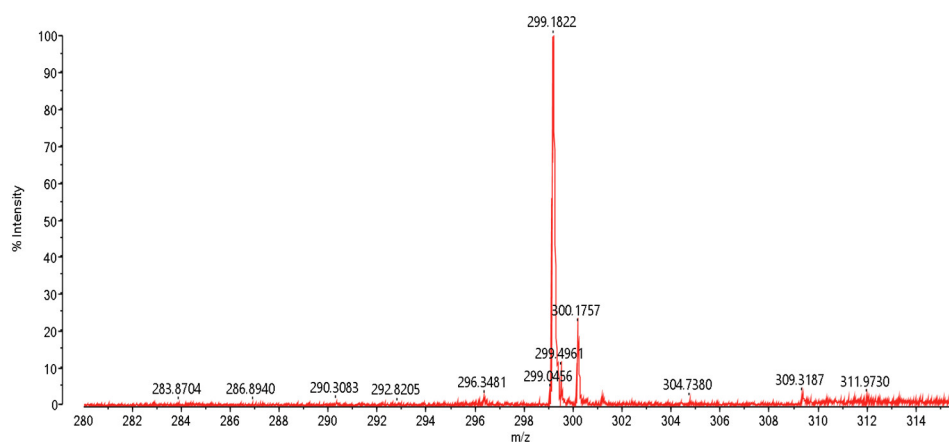
Figure S2. The MALDI-TOF Mass Spetrum of CNPTEG.

MALDI-TOF MS was calculated for C$_{14}$H$_{16}$N$_2$O$_4$ 276.1110, found 299.1822. (M + Na$^+$).
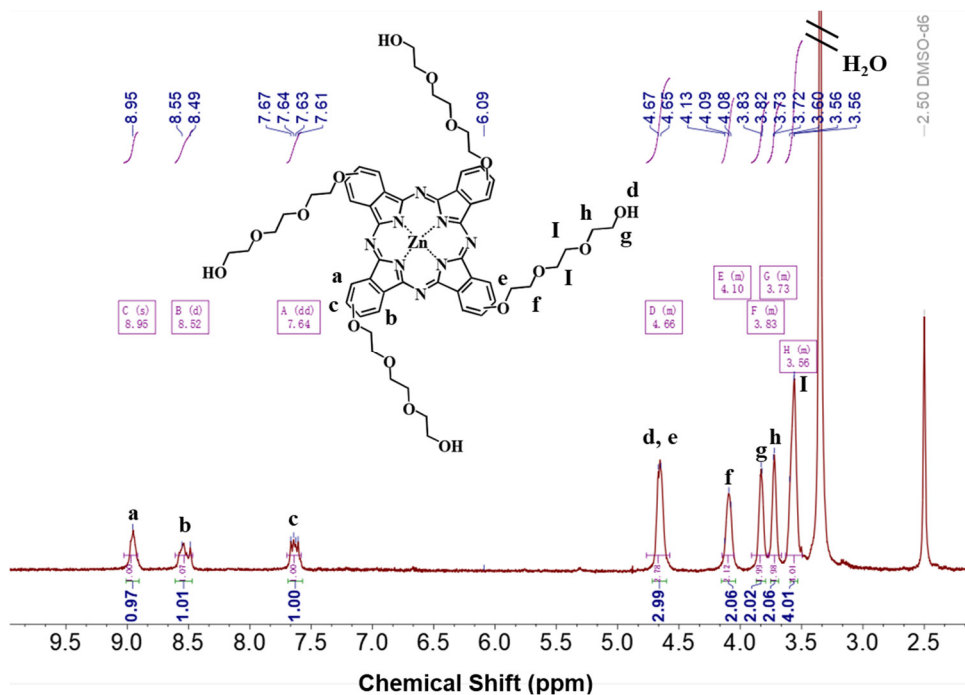
Figure S3. The ^{1}H NMR spectrum of ZnPc-TEG (DMSO-d_6, 400 MHz).

^{1}H NMR (400 MHz, DMSO-d_6): δ 8.95 (s, 4H), 8.52 (d, J = 9.3 Hz, 4H), 7.64 (dd, J = 15.0, 8.4 Hz, 4H), 4.76 – 4.57 (m, 12H), 4.15 – 4.05 (m, 8H), 3.91 – 3.77 (m, 8H), 3.78 – 3.66 (m, 8H), 3.63 – 3.49 (m, 16H).
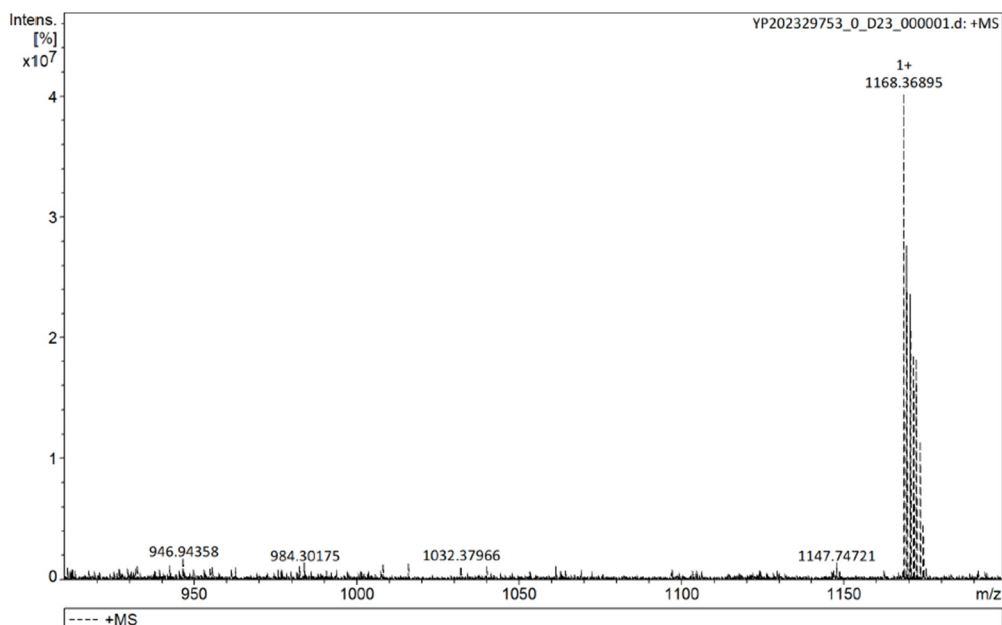
Figure S4. The MALDI-TOF Mass Spectrum of ZnPc-TEG.

MALDI-TOF MS was calculated for $C_{56}H_{64}N_8O_{16}Zn$ 1168.3732, found 1168.3690 (M$^+$).

Acquisition Parameter

Source Type	ESI	Ion Polarity	Positive	Set Nebulizer	2.0 Bar
Focus	Active	Set Capillary	4500 V	Set Dry Heater	220 °C
Scan Begin	50 m/z	Set End Plate Offset	-500 V	Set Dry Gas	8.0 l/min
Scan End	1300 m/z	Set Charging Voltage	2000 V	Set Divert Valve	Waste
		Set Corona	0 nA	Set APCI Heater	0 °C

dy-0915-znpc_1-12_01_17879.d: +MS, 0.5min #57

Meas. m/z	#	Ion Formula	m/z	Sum Formula	err [ppm]	mSigma	# mSigma	Score	rdb	e⁻ Conf	N-Rule
1191.3618	1	C56H64N8NaO16Zn	1191.3624	C56H64N8O16Zn	0.5	173.6	1	100.00	29.0	even	ok
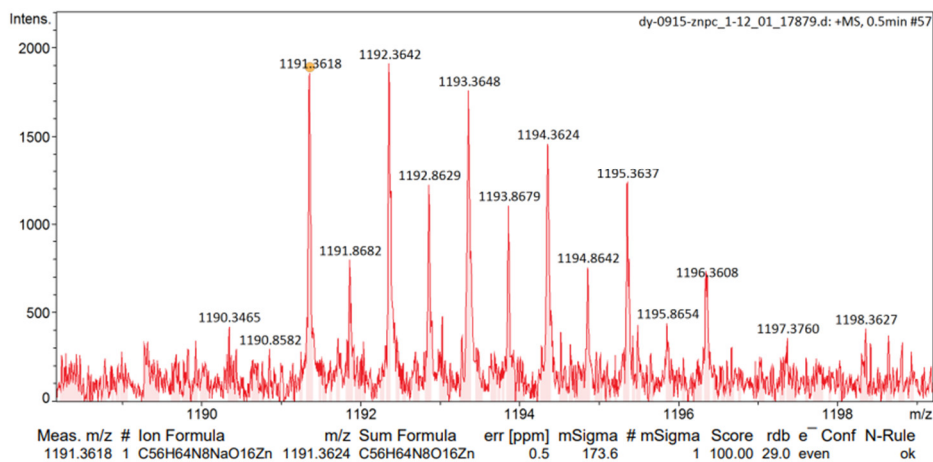
Figure S5. The Mass Spectrum of ZnPc-TEG in the ESI.
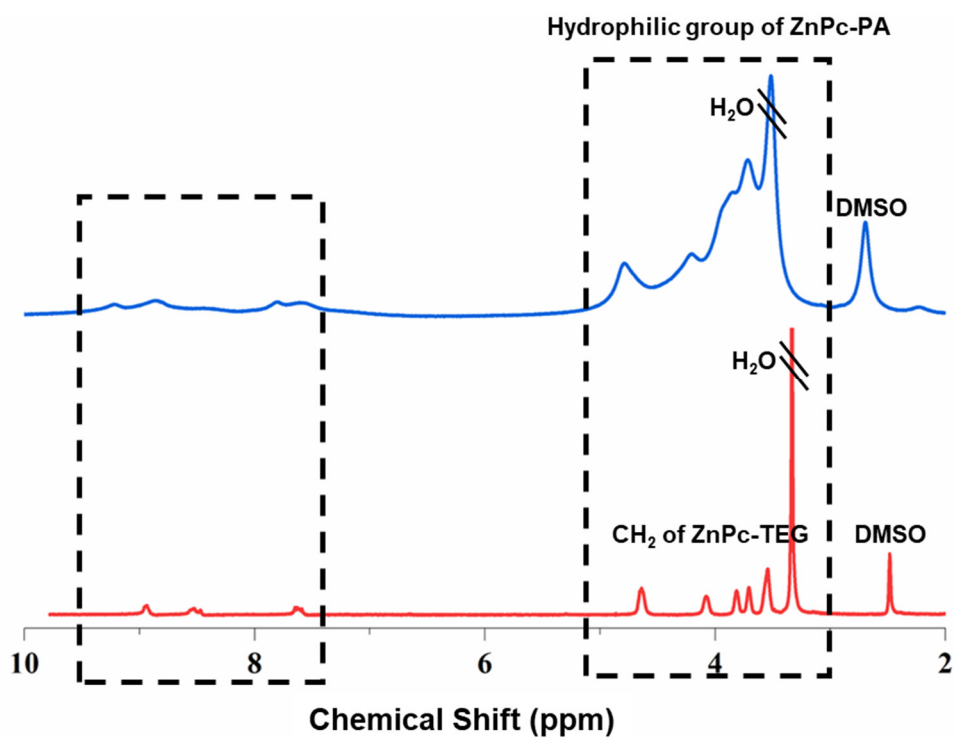
Figure S6. The ^{1}H NMR spectrum of ZnPc-PA (DMSO-d_6, 400 MHz).
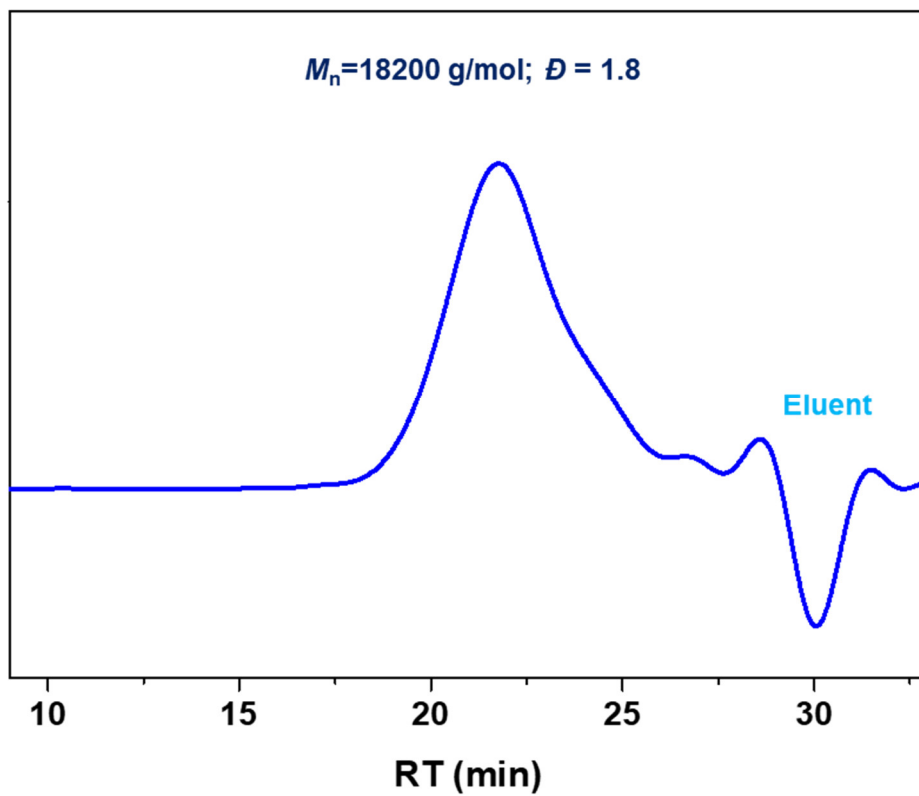
Figure S7. The Gel Permeation Chromatography of ZnPc-PA.
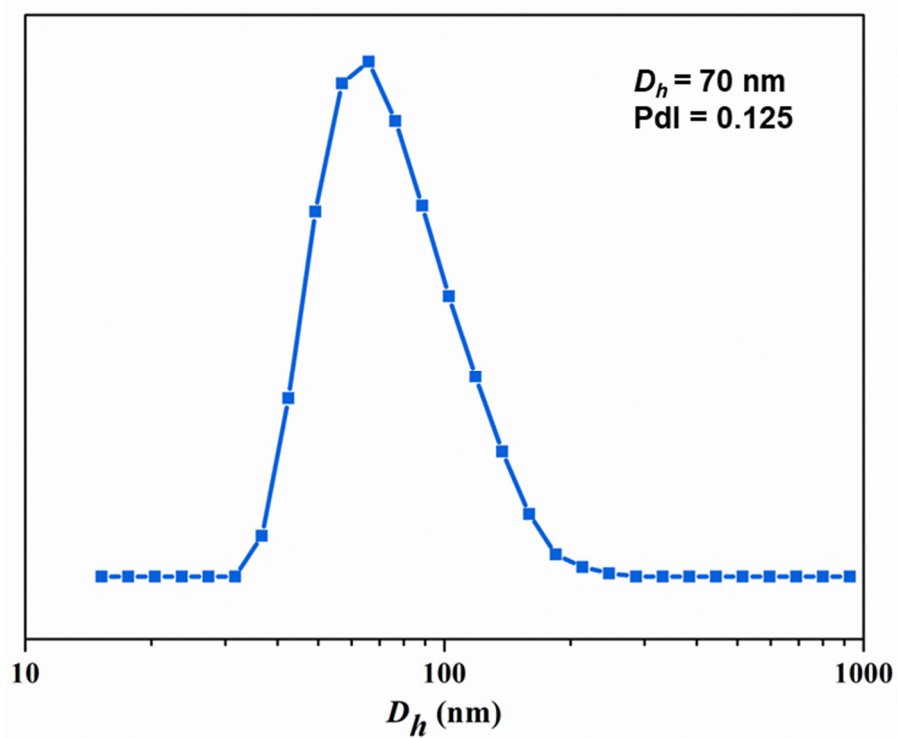
Figure S8. The D_h of ZnPc-PA micelles.
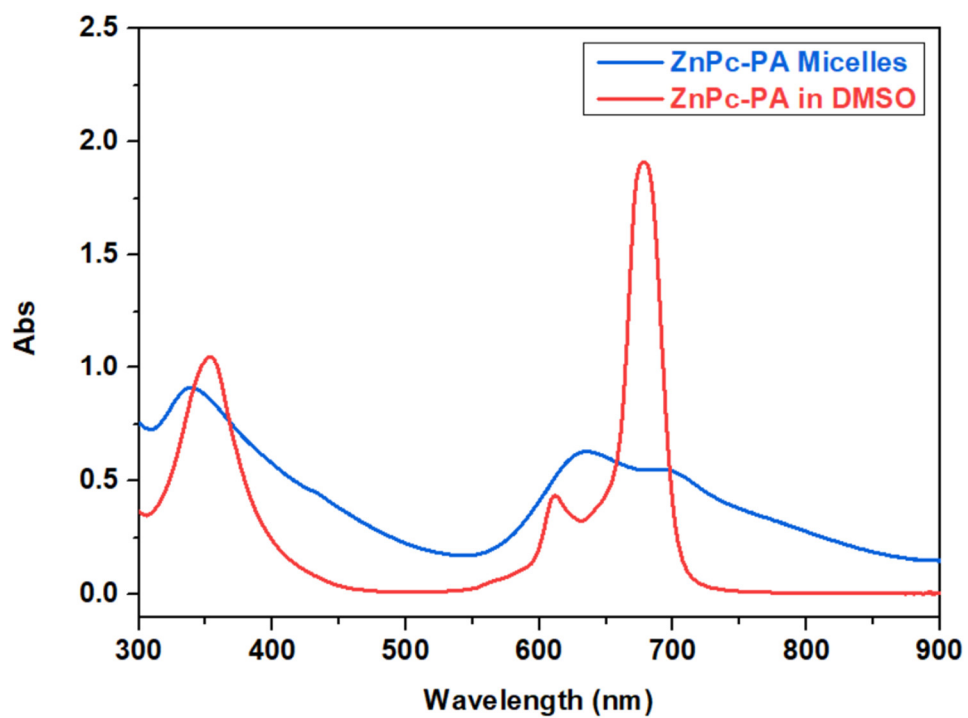
Figure S9. UV-vis absorption spectra of ZnPc-PA/DMSO solution and ZnPc-PA micelle aqueous solution.
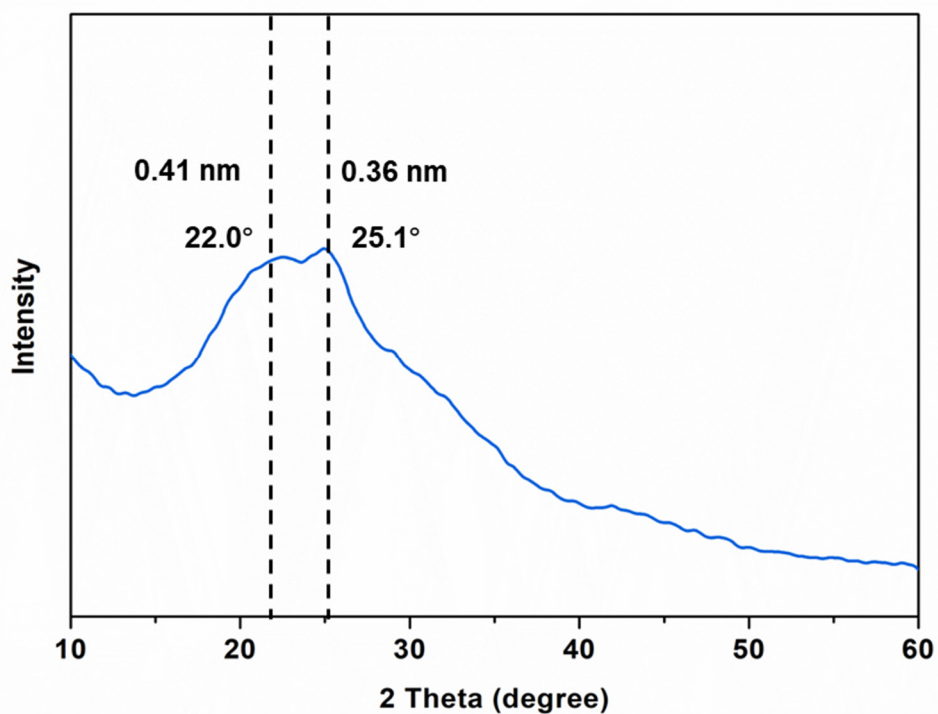
Figure S10. The powder X-Ray diffraction of ZnPc-PA micelles after drying.
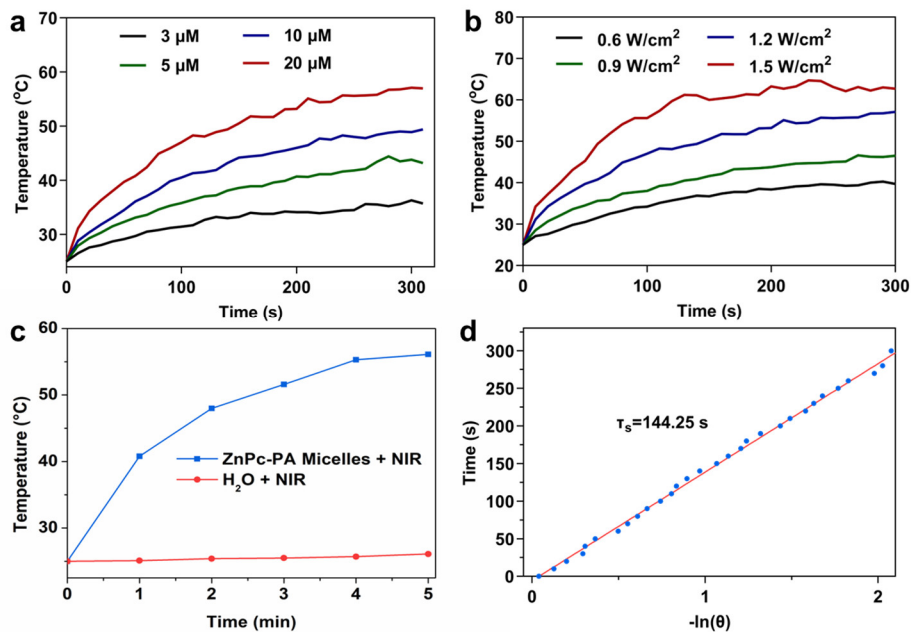
Figure S11. Temperature variation of ZnPc-PA micelle aqueous solution at different concentrations (a) and different intensities (b). (c) Temperature changes of H_2O and ZnPc-PA micelles (20 μM) under an 808 nm laser (1200 mW/cm^2). (d) Linear fitting curve of the cooling time of ZnPc-PA micelle solution as a function of negative logarithm of temperatures.
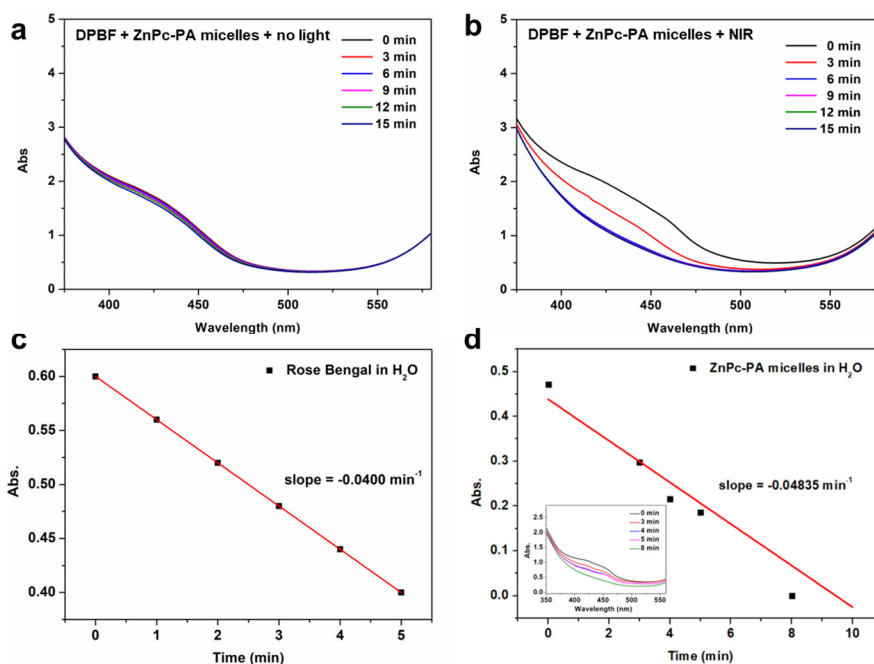
Figure S12. (a, b) ROS detection of ZnPc-PA micelles. UV-vis absorption spectra of DPBF in ZnPc-PA micelle solution (20 μM) without light (a) and with 808 nm laser irradiation (1200 mW/cm^2) (b) at different time (0, 3, 6, 9, 12, 15 min). (c) The absorbance decay curves of DPBF for Rose Bengal (RB, Φ_Δ (H_2O) = 0.75) with 808 nm laser irradiation (1200 mW/cm^2). (d) The absorbance decay curves of DPBF for ZnPc-PA micelle solution with 808 nm laser irradiation (1200 mW/cm^2) (Inset: UV-vis absorption spectra of DPBF in ZnPc-PA micelle solution with 808 nm laser irradiation at different time).
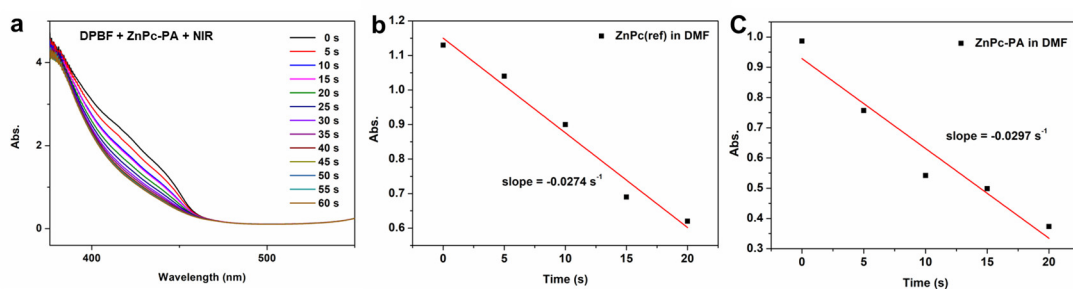
Figure S13. (a) UV-vis absorption spectrum of DPBF in micellar-free ZnPc-PA/DMF solution (20 μM) with 808 nm laser irradiation (1200 mW/cm^2) at different time. (b) The absorbance decay curves of DPBF for unsubstituted zinc (II) phthalocyanine (ZnPc, $\Phi_\Delta = 0.56$) in DMF with 808 nm laser irradiation (1200 mW/cm^2). (c) The absorbance decay curves of DPBF for ZnPc-PA in DMF with 808 nm laser irradiation (1200 mW/cm^2).
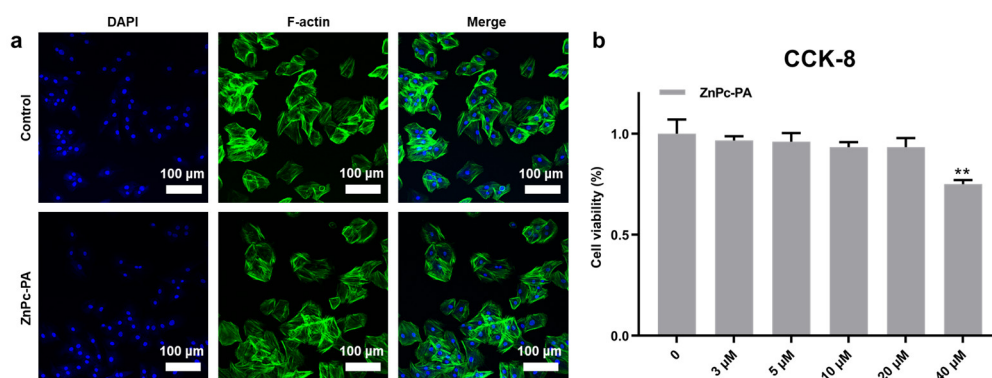
Figure S14. Cytotoxic evaluation of ZnPc-PA micelles. (a) Cell morphologies of ECV304 cells after incubation with PBS (control) and ZnPc-PA for 24 hours. (b) Assessment of cell viability by CCK-8 assay after co-incubation with ZnPc-PA at various concentrations on day 1 (n = 3, **P < 0.01).
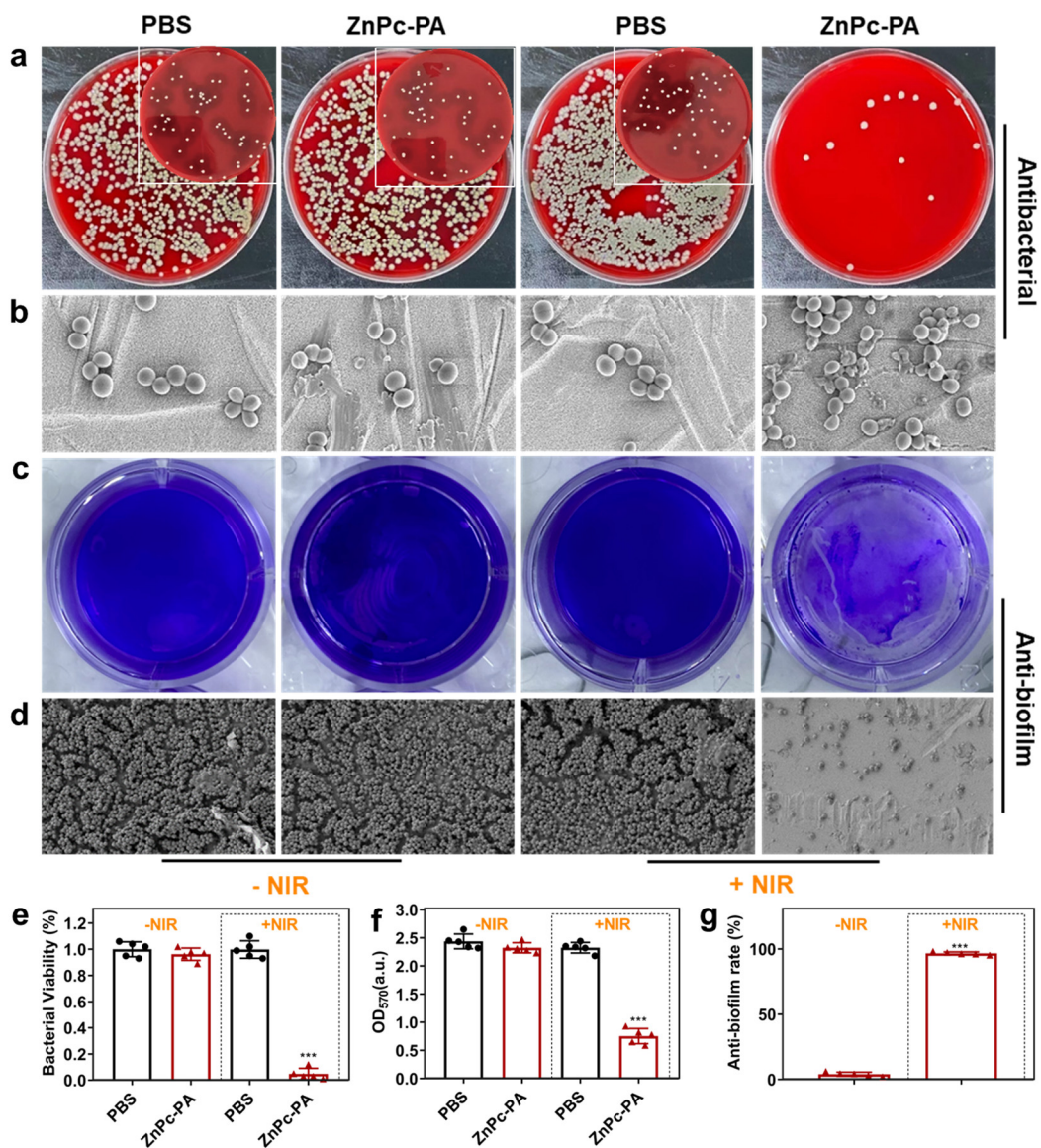
Figure S15. *In vitro* antibacterial and anti-biofilm effects. a) Colony-forming units (CFUs) on sheep blood agar plates of MRSA after treatment with PBS and ZnPc-PA micelles (20 μM) with NIR laser irradiation (1200 mW/cm^2) for 5 minutes, respectively. Insets: 10-fold dilution. b) SEM images of MRSA coli after various treatments, respectively. c) Crystal violet staining images of MRSA on the surface of a Ti disk in different groups. d) SEM images of MRSA-biofilm on the surface of a Ti disk in different groups. e) Bacterial viability of MRSA based on CFU counts for the above groups. (n = 5, *** p < 0.001). f) Crystal violet staining of MRSA on the surface of a Ti disk in different groups. g) Anti-biofilm rate of NIR-activated ZnPc-PA micelles according to CFUs on surface of a Ti disk. (n = 5, *** p < 0.001).
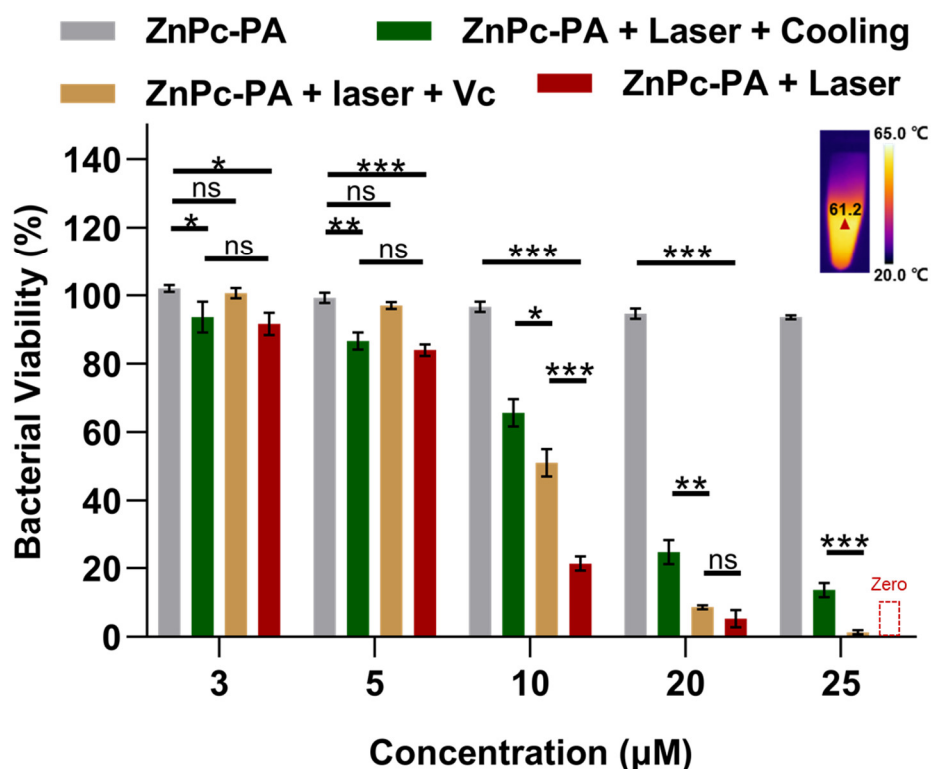
Figure S16. The photocytotoxicity of ZnPc-PA micelles on MRSA. Inset shows the thermal images of ZnPc-PA micelle (25 μM) at 1200 mW/cm^2 for 5 min. It was found bacterial viability was reduced in a ZnPc-PA micelle concentration-dependent manner, and both PDT and PTT effects on antibacterial activity increased with increasing ZnPc-PA micelle concentration. PDT was predominant the antibacterial activity, albeit on mild effect, when ZnPc-PA micelles were at a concentration of 3 or 5 μM. Instead, PTT was more effective than PDT when the concentration was above 10 μM. When ZnPc-PA micelle was at 25 μM, the antibacterial rate was 94.7% for PTT and 78.7% for PDT, respectively. However, such a high ZnPc-PA micelle concentration would induce hyperthermia above 60 °C (inset), a potential risk to healthy tissues. Therefore, ZnPc-PA micelle at 20 μM was chosen for the biological experiments. In this selected concentration, the antibacterial rate was 91.3% for PTT and 75.3% for PDT, respectively.
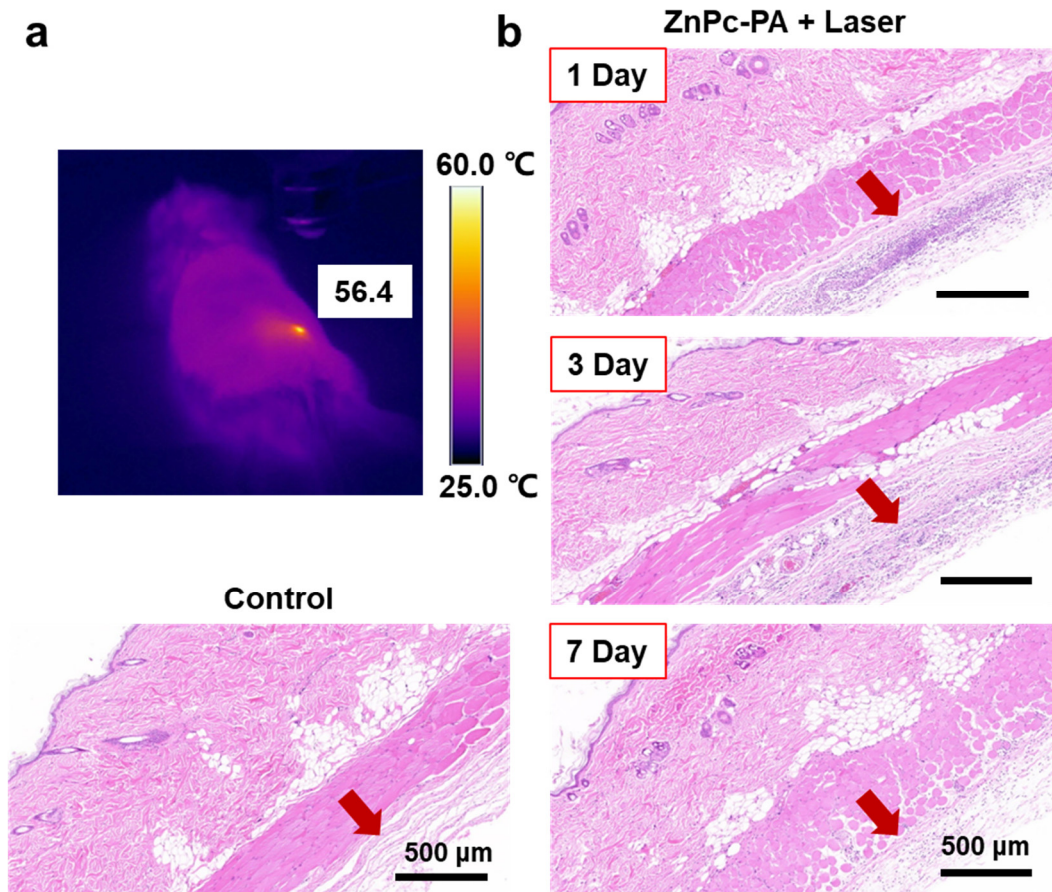
Figure S17. The effect of laser-activated ZnPc-PA micelles on healthy tissue. (a) Real-time record of temperature triggered by ZnPc-PA micelles (20 μM) with 808 nm laser at 1200 mW/cm^2 for 5 min. (b) H&E staining showing local inflammatory responses on Day 1, 3 and 7 after treatments. Red arrows indicate inflammatory sites.
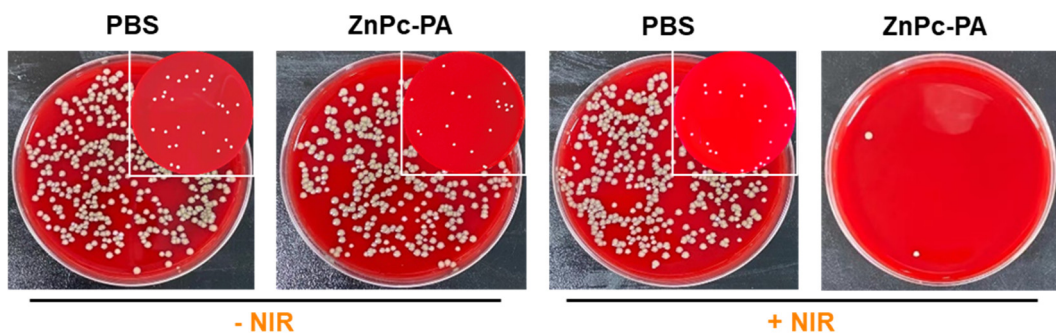
Figure S18. Bacterial colonies obtained by the spreading plate method from the biofilms on the retrieved Ti implants when the *in vivo* experiments were terminated. Insets: 10-fold dilution.

1. X. Li, C. Y. Kim, S. Lee, D. Lee, H. M. Chung, G. Kim, S. H. Heo, C. Kim, K. S. Hong and J. Yoon, *J. Am. Chem. Soc.*, 2017, **139**, 10880–10886.
2. J. Wang, R. M. Wolf, J. W. Caldwell, P. A. Kollman and D. A. Case, *J. Comput. Chem.*, 2004, **25**, 1157–1174.
3. L. Martinez, R. Andrade, E. G. Birgin and J. M. Martinez, *J. Comput. Chem.*, 2009, **30**, 2157–2164.
4. H. J. C. Berendsen, D. van der Spoel, R. van Drunen, *Comput. Phys. Commun.*, 1995, **91**, 43–56.
5. G. J. Martyna, M. L. Klein and M. Tuckerman, *J. Chem. Phys.*, 1992, **97**, 2635–2643.
6. G. J. Martyna, D. J. Tobias and M. L. Klein, *J. Chem. Phys.*, 1994, **101**, 4177–4189.
7. M. Parrinello and A. Rahman, *J. Appl. Phys.*, 1981, **52**, 7182–7190.
8. Y. Liu, H. Wang, S. Li, C. Chen, L. Xu, P. Huang, F. Liu, Y. Su, M. Qi, C. Yu and Y. Zhou, *Nat. Commun.*, 2020, **11**, 1724.
9. C. Chen, G. Chu, W. He, Y. Liu, K. Dai, J. Valdez, A. Moores, P. Huang, Z. Wang, J. Jin, M. Guan, W. Jiang, Y. Mai, D. Ma, Y. Wang and Y. Zhou, *Adv. Mater.*, 2023, **35**, e2207950.
10. A. Galstyan, A. Ricker, H. Nüsse, J. Klingauf and U. Dobrindt, *ACS Appl. Bio Mater.*, 2019, **3**, 400–411.
11. M. Tavakkoli Yaraki, B. Liu and Y. N. Tan, *Nano-Micro Lett.*, 2022, **14**, 123.
12. M. Li, C. Yu, C. Hu, W. Yang, C. Zhao, S. Wang, M. Zhang, J. Zhao, X. Wang and J. Qiu, Chem. Eng. J., 2017, **320**, 570–575.